Bull Mater Sci (2020) 43:254
https://doi.org/10.1007/s12034-020-02218-z

Preparation and characterization of Guar gum-based solid biopolymer electrolyte doped with lithium bis(trifluoromethanesulphonyl)imide (LiTFSI) plasticized with glycerol

M ABIRAMI, R SARATHA, R SHILPA* and B VINITHA
Department of Chemistry, Avinashilingam Institute for Home Science and Higher Education for Women, Coimbatore 641043, India
*Author for correspondence (6789shilpa@gmail.com)

MS received 21 November 2019; accepted 25 March 2020

Abstract. The Guar gum (GG)–lithium bis(trifluoromethanesulphonyl)imide (LiTFSI)-glycerol-based solid biopolymer electrolyte has been investigated. The polymer electrolytes has been prepared *via* solution casting technique and characterized by Fourier transform infrared (FTIR), X-ray diffraction (XRD), thermogravimetric analysis (TGA), 3D-laser profilometry and AC impedance studies. The amorphous nature and complexation has been revealed by XRD and FTIR. TGA reveals that the polymer electrolyte is stable up to 260°C. The average roughness was measured using 3D-laser profilometry. The ionic conductivity of the electrolyte was studied using impedance analysis. The best optimum ionic conductivity of 2.041×10^{-3} S cm^{-1} has been achieved for the film containing 60 wt% GG–40 wt% LiTFSI.

Keywords. Biopolymer; LiTFSI; XRD; FTIR; TGA; AC impedance studies.

1. Introduction

Throughout the recent past, solid polymer electrolytes (SPEs) i.e., polymer–salt complexes have gained more attention owing to their potential applications in many electrochemical devices for example batteries, chemical sensors, photo-electrochemical cells, smart windows etc. SPEs have numerous advantages such as mechanical strength, free from leakage, good electrode–electrolyte contact, ease of fabrication into thin film, electrochemical stability and high energy density [1–4]. Moreover, the limitations of liquid electrolytes (poor chemical stability, reaction with electrodes and leakage) can overcome by SPEs [5]. A number of SPEs have been synthesized and characterized using synthetic polymers that include PVdF-HFP, PMMA, PAN, PEO, PPO, PEG etc. [6,7].

Currently, our globe is facing many challenges as a result of the environmental issues. On the other hand, synthetic polymers also pose challenges like high cost, non-biodegradability and insolubility in solvents [3,5]. Research studies have focussed on biopolymer electrolytes which are obtained from natural polymers. Natural polymers can overcome many challenges due to their non-toxicity, abundance in nature, eco-friendliness, renewability and biodegradability [8]. Ahmad Khiar and Arof [9] reported conductivity of 2.83×10^{-5} S cm^{-1} for starch/NH_4NO_3 system. The carboxymethyl cellulose/NH_4Br system was prepared by Samsudin and Saadiah [10] and achieved conductivity of 3.31×10^{-3} S cm^{-1}. The conductivity of 6.1×10^{-4} S cm^{-1} was obtained for I-carrageenan/magnesium nitrate system [11]. The conductivity of 2.08×10^{-3} S cm^{-1} for pectin/LiCl system was reported by Perumal *et al* [12]. The conductivity was found to be $(1.51 \pm 0.12) \times 10^{-3}$ S cm^{-1} for chitosan/NH_4SCN system [13]. Sit *et al* [14] reported conductivity of 3.61×10^{-4} S cm^{-1} for the complex formation of hydroxymethyl cellulose with NH_4Br salts. The conductivity of 2.7×10^{-4} S cm^{-1} for chitosan/$LiNO_3$ system was reported by Mohamed *et al* [15]. GG, a polysaccharide, belongs to the family of galactomannans and it is derived from the refined endosperm of cluster bean seeds [16]. From the literature survey, it has been found that GG is used as a binder [17–19], gel polymer electrolyte [20] and there is no evidence for GG use as a solid biopolymer electrolyte. The properties of polymer electrolytes including amorphous nature, thermal stability and conductivity may also be influenced by incorporating salts into the polymer matrix [12]. Lithium salts are typically chosen as a doping salt, because lithium being the lightest of all metals also has a large potential window [21]. Some of the lithium salts that are used in SPEs are lithium hexafluorophosphate ($LiPF_6$) [22], lithium triflate ($LiCF_3SO_3$) [23], lithium chloride (LiCl) [24],

Published online: 03 September 2020

lithium 4,5-dicyano-2-(trifluoromethyl)imidazole [25], lithium perchlorate ($LiClO_4$) [26] and lithium nitrate ($LiNO_3$) [27]. Among the various lithium salts, lithium bis(trifluoromethanesulphonyl)imide (LiTFSI) has been selected as the doping salt owing to its electronegativity, flexibility and bulky delocalization of charges [28]. In this present work, we study biopolymer GG complexed with different concentrations of LiTFSI and plasticized with glycerol. The polymer membranes were characterized by various techniques. The new combination of the polymer and salt and its biodegradability shows the novelty of this study.

2. Experimental

2.1 *Materials used*

Biopolymer GG (host polymer), LiTFSI (doping salt), glycerol (plasticizer) and distilled water (solvent) were used.

2.2 *Synthesis of polymer films*

Biopolymer GG–LiTFSI complex membranes were prepared using solution casting method. GG and various compositions of LiTFSI (80:20, 70:30, 60:40 and 50:50 molecular weight percentage of GG:LiTFSI) were dissolved in distilled water. A volume of 0.2 ml glycerol was added to each composition. In order to obtain homogeneous solutions, the mixture was stirred using a magnetic stirrer for about 24 h at room temperature. The solutions were then cast into Petri dishes and placed in a hot air-oven at constant temperature of 40°C for 24 h to evaporate the solvent.

2.3 *Characterization*

The Fourier transform infrared (FTIR) spectra of the pure GG and LiTFSI doped GG samples were obtained using FTIR (Miracle 10 Shimadzu) spectrophotometer in the frequency range of 400–4000 cm^{-1} at room temperature. X-ray diffraction (XRD) patterns of the polymer membranes were recorded using XPERT PRO Diffractometer in the range of 2θ = 10–90° at room temperature. The samples were cut into 2 × 2 cm^2 and placed between two stainless steel blocking electrodes. Using HIOKI 3532-50 LCR HITESTER, the impedance measurements were carried out at room temperature in the frequency range of 42 Hz to 1 MHz. The thermogravimetric analyses (TGA) were performed by TG/DTA 6300 Model instrument from EXSTAR. The average roughness of the samples can be calculated using 3D Optical Profilo Meter (Zeta-20).

3. Results and discussion

3.1 *FTIR spectroscopy*

FTIR spectra of pure GG, LiTFSI and GG–LiTFSI polymer electrolytes are shown in figure 1. In pure GG, the O–H stretching at 3278 cm^{-1} [29] is widened which shows the interaction of functional groups upon the addition of lithium salt which clearly manifest the major shifting of the peaks such as 3325 cm^{-1} (80:20 wt%), 3379 cm^{-1} (70:30 wt%), 3541 cm^{-1} (60:40 wt%) and 3564 cm^{-1} (50:50 wt%) in the doped samples. The other important peak at 2931 cm^{-1} corresponds to the C–H stretching mode.

The peaks between 800 and 1200 cm^{-1} are observed for highly coupled C–C–O, C–OH and C–O–C stretching modes of polymer backbone [29]. The peaks at 779 and 902 cm^{-1} show the (1–4) and (1–6) linkages of galactose and mannose in the pure GG. The characteristic peak of galactose and mannose at 871 cm^{-1} is observed for pure GG which is shifted towards 864 cm^{-1} for the doped samples.

The spectra of LiTFSI exhibit two weak peaks at 740 and 820 cm^{-1}. The former peak corresponds to S–N stretching mode, whereas the latter peak is the combination of C–S stretching and S–N asymmetric stretching mode [30]. The former peak has appeared in the doped samples whereas the latter peak shows shift in the linkages. A medium peak, namely the S=O asymmetric stretching mode of LiTFSI is attained at 1319 cm^{-1} which undergoes a shift towards 1342 cm^{-1}.

LiTFSI spectrum denotes a sharp peak at 1058 cm^{-1} (assigned as S–N–S asymmetric stretching mode of LiTFSI) which was observed at 1049 cm^{-1} for the other samples. LiTFSI spectrum displays two peaks at 1134 and 1195 cm^{-1}. The first peak is assigned as the combination of C–F stretching mode and C–SO_2–N bonding mode of LiTFSI. CF_3 symmetric stretching mode of LiTFSI is assigned for

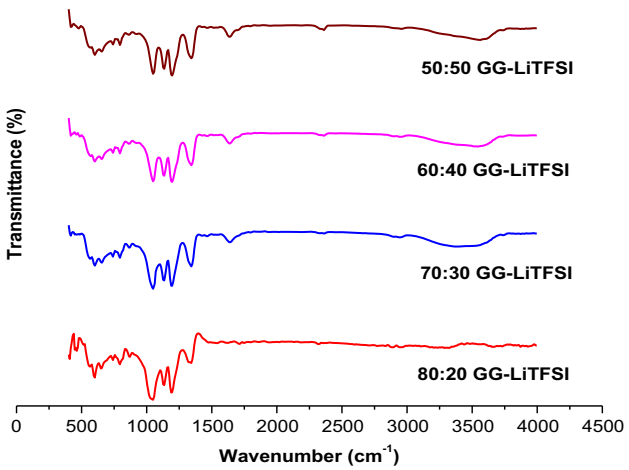

Figure 1. FTIR spectra of pure GG, LiTFSI and GG–LiTFSI polymer electrolytes.

Table 1. Peak assignments of pure GG, LiTFSI and GG–LiTFSI polymer electrolytes.

Peak/band assignments	Wavenumber (cm^{-1})					
	GG	LiTFSI	80:20 wt%	70:30 wt%	60:40 wt%	50:50 wt%
O–H stretching	3278	—	3325	3379	3541	3564
C–H stretching of CH_2 group	2931	—	2954	2947	2954	2954
CF_3 symmetric stretching mode of LiTFSI	—	1195	1188	1195	1195	1195
S=O asymmetric stretching mode of LiTFSI	—	1319	1342	1342	1342	1342
S–N–S asymmetric stretching mode of LiTFSI	—	1056	1049	1049	1049	1049
Combination of C–F stretching mode and C–SO_2–N bonding mode of LiTFSI	—	1134	1134	1134	1134	1134
(1–4), (1–6) linkages of galactose and mannose	779,902	—	794	794	794,925	794,918
Galactose and mannose	871	—	871	864	864	864
S–N stretching mode of LiTFSI	—	740	740	740	740	740
Combination of C–S stretching and S–N asymmetric stretching mode	—	802	—	—	—	—

the second peak. The peak assignments of pure GG, LiTFSI and GG–LiTFSI polymer membranes are listed in table 1.

3.2 *X-ray diffraction (XRD)*

Figure 2 shows the XRD pattern of pure GG and GG doped with different compositions of LiTFSI. For pure GG, low crystallinity is observed and its crystalline region is found at an angle 2θ = 20.02°. A similar result was reported by Mudgil *et al* [29]. The relative intensity of broad peak is observed between 15 and 25°. As the concentration of the ionic dopant (LiTFSI) increases, the intensity of the broad peak decreases, and this is possible only if there is an interaction between the polymer and the salt. As a result, amorphousness and the conductivity increase in the polymer membranes. The peaks corresponding to LiTFSI are not observed in all four GG–LiTFSI polymer electrolytes which revealed a complete dissociation of salt in the polymer electrolyte. This result can be understood by Hodge *et al* [31] criterion, which forms a relationship between the degree of crystallinity and the intensity of the peak. When 50 wt% of LiTFSI is added, there is a decrease in conductivity of the polymer matrix. This may be due to the recrystallization of the salt [32]. The polymer electrolyte of GG containing 60:40 wt% GG–LiTFSI exhibits maximum amorphous nature.

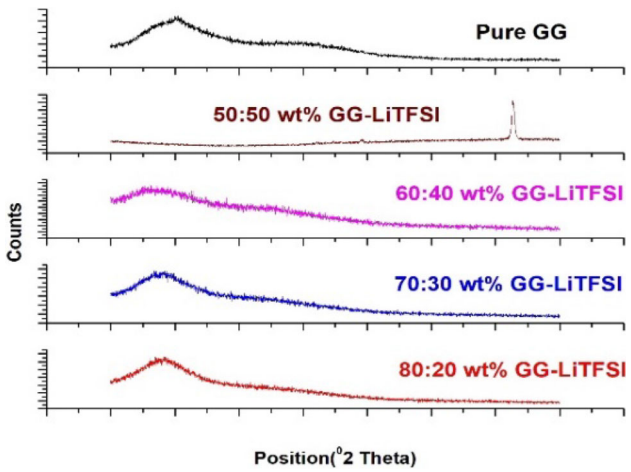

Figure 2. XRD pattern of pure GG and GG–LiTFSI polymer electrolytes.

3.3 *Thermogravimetric analysis (TGA)*

Figure 3 shows TG curve of pure GG and various compositions of GG–LiTFSI polymer electrolytes. For native GG, the initial weight loss of 13.8% at 86°C is due to the degradation of entrapped moisture content. With a further increase in temperature, a major weight loss of 60% at 250°C is observed.

For 80:20 wt% GG–LiTFSI polymer electrolyte, the weight loss of 17.8% at 244°C takes place in the first region. This mass loss is due to the evaporation of residual moisture

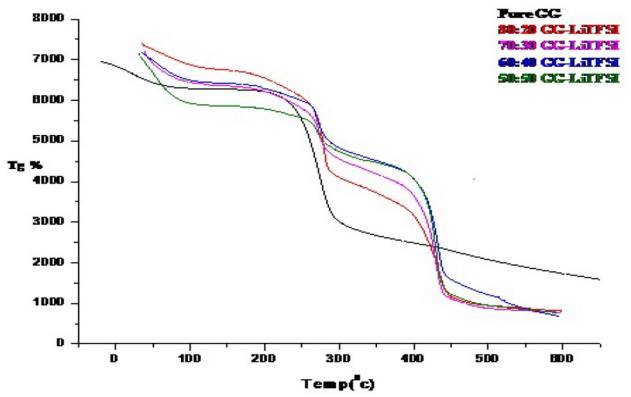

Figure 3. TG curve of pure GG and GG–LiTFSI polymer electrolytes.

content in the sample. Beyond this region, a major weight loss of 34% is observed. The degradation can be attributed to the cleavage of C–O–C bonds in galactose and mannose backbones, resulting in CO_2 elimination from the GG backbone [29]. A similar weight loss is observed in the second region for 70:30, 60:40 and 50:50 wt% GG–LiTFSI polymer electrolytes such as 27.3, 27.7 and 20.6% at 260, 263 and 261°C respectively. From TGA results, it can be concluded that on adding plasticizer and dopant the thermal stability of polymer membranes was significantly affected [16].

3.4 *3D-laser profilometry analysis*

The surface features and topography of surface of polymer electrolyte are studied using a 3D-laser profilometer. It has been found that as the R_a value increases, the roughness of the sample surface increases. The comparison of R_a values for different concentrations of polymer membranes are shown in table 2.

From the R_a values, it is found that among the four prepared polyelectrolyte thin films, 80:20 and 70:30 wt% show lower R_a value of about 3.64 and 10.9% respectively. Thus these two concentrations of GG–LiTFSI polyelectrolyte thin films were comparatively smoother than the other two concentrations such as 60:40 wt% and 50:50 wt% which possess higher R_a values of 26.1 and 54.2% (figure 4).

Table 2. R_a (average roughness) values for GG–LiTFSI polymer electrolytes.

Composition of GG–LiTFSI polymer electrolyte (wt%)	R_a values (%)
80:20	3.64
70:30	10.9
60:40	26.1
50:50	54.2

3.5 *AC impedance studies*

Electrochemical impedance spectroscopy is the most powerful tool for characterizing the electrical properties of the polymer matrix. The semi-circle can be represented by a parallel combination of a capacitor, which is due to the immobile polymer chain. As the salt concentrations begin to increase, it was observed that the semi-circle in the plots lessened and finally left only a low-frequency spike. This suggests that only the resistive component of the polymer electrolytes exists which is due to the mobile ions inside the polymer matrix. The factors which influence the ionic conductivity of polymer electrolytes are types of charge carriers (cationic or anionic), temperature and ionic conducting species. The Cole–Cole plot for GG incorporated with different concentrations of LiTFSI at room

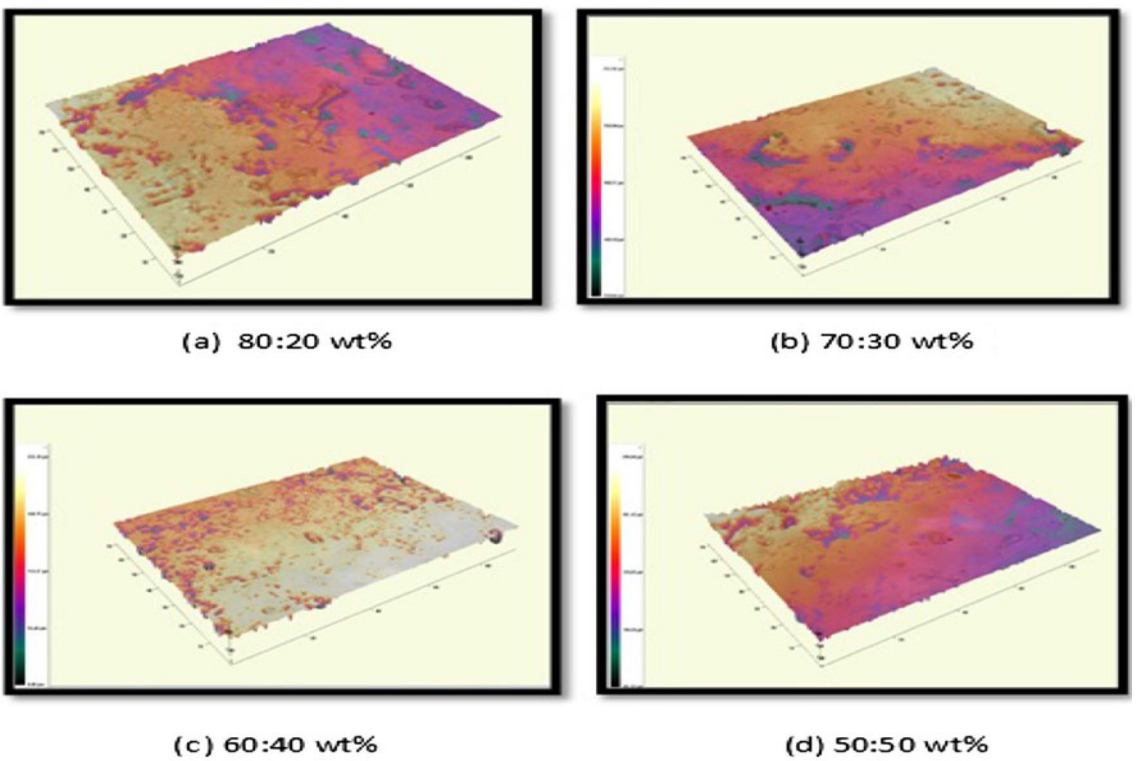

Figure 4. Zeta 3D images of GG–LiTFSI polymer electrolytes.

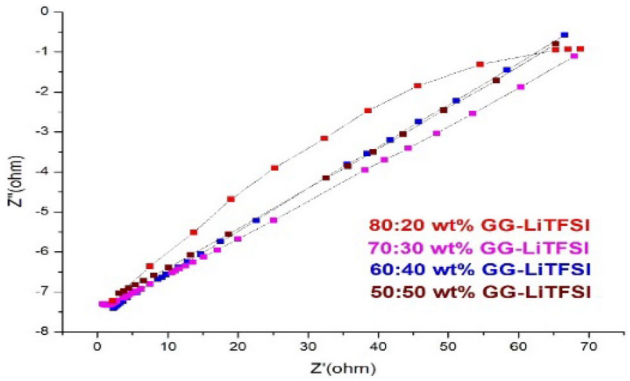

Figure 5. Cole–Cole plot for GG–LiTFSI polymer electrolytes.

Table 3. Ionic conductivities of GG doped with different wt% of LiTFSI.

Composition of GG–LiTFSI polymer electrolytes (wt%)	Ionic conductivity (S cm^{-1})
80:20	8.862×10^{-6}
70:30	4.150×10^{-5}
60:40	2.0416×10^{-3}
50:50	8.305×10^{-3}

temperature (303 K) is shown in figure 5. In the impedance curve, the absence of semi-circle indicates the transport of ions across electrode–electrolyte interface which is the main reason for conductivity [33]. The bulk resistance R_b can be measured from the low frequency spike intercept on the Z' axis. The conductivity values of the polymer membranes can be measured using the below equation:

$$\sigma = l/AR_b\,(\mathrm{S\,cm^{-1}})$$

where l is the thickness of the film, A is the surface area of the electrolyte and R_b is the bulk resistance.

From table 3, it is concluded that the film containing 60 GG:40 LiTFSI exhibited the highest ionic conductivity of order 2.041×10^{-3} S cm^{-1}. On increasing the salt concentration (50 wt%), the conductivity is found to decrease owing to the aggregation of ions. The aggregation of salt in the polymer membrane is due to the re-association of anions and cations [34]. This aggregation suppresses the number of density of free mobile ions, which in turn decreases the conductivity [33].

3.5a *Conductance spectra analysis:* The conductance spectra for different wt% of LiTFSI doped with GG at 303 K (room temperature) are shown in figure 6. Generally, the conductance spectra show three distinct regions namely low frequency dispersion region, frequency independent plateau region and high frequency dispersion region. The low frequency region occurs due to the phenomenon of electrode–electrolyte interface. The DC conductivity can

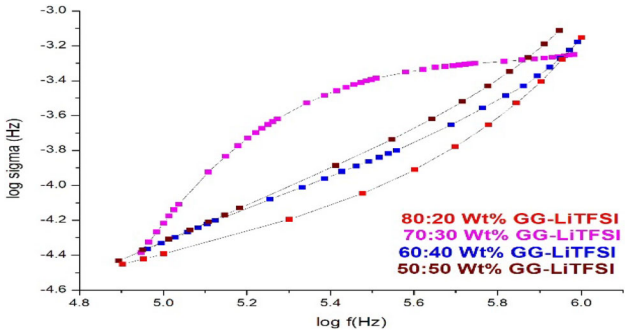

Figure 6. Conductance spectra of GG–LiTFSI polymer electrolytes.

be attained by extrapolating the plateau region to the Y-axis (zero frequency) which correlates with the values obtained from the Cole–Cole plot. The high frequency corresponds to the bulk relaxation phenomenon. It is found that as the concentration of LiTFSI increases, the σ_{DC} increases up to 40 wt%.

4. Conclusion

A new GG-based solid biopolymer electrolyte doped with LiTFSI has been synthesized *via* the solution casting method. The complexation between host polymer and doping salt was confirmed by FTIR. XRD studies confirm the amorphous nature of the prepared SPEs. The prepared SPEs are thermally stable up to 260°C. From 3D laser profilometry, it can be concluded that the samples (80:20 and 70:30 wt%) are comparatively smoother than the other two samples. The highest ionic conductivity of 2.041×10^{-3} S cm^{-1} has been attained for the film containing 60 wt% GG–40% wt% LiTFSI.

References

[1] Jaipal Reddy M, Chu P P, Sreekanth T and Subba Rao U V 2001 *J. Mater. Sci.: Mater. Electron.* **12** 153
[2] Ou R, Xie Y, Shen X, Yuan F, Wang H and Wang Q 2012 *J. Mater. Sci.* **47** 5978
[3] Ma X, Yu J, He K and Wang N 2007 *Macromol. Mater. Eng.* **292** 503
[4] Pradhan D K, Choudhary R N P, Samantaray B K, Karan N K and Katiyar R S 2007 *Int. J. Electrochem. Sci.* **2** 861
[5] Rani M S A, Dzulkurnaina N A, Ahmadb A and Mohamed N S 2015 *Int. J. Polym. Anal. Charact.* **20** 250
[6] Manuel Stephan A 2006 *Eur. Polym. J.* **42** 21
[7] Christopher Selvin P, Perumal P, Selvasekarapandian S, Monisha S, Boopathi G and Leena Chandra M V 2018 *Ionics*
[8] Emo Chielhi and Roberto Solaro 1996 *Adv. Mater.* **8** 305
[9] Ahmad Khiar A S and Arof A K 2010 *Ionics* **16** 123
[10] Samsudin A S and Saadiah M A 2018 *J. Non-Cryst. Solids* **497** 19

[11] Shanmuga Priya S, Karthika S, Selvasekarapandian S and Manjuladevi R 2018 *Solid State Ionics* **327** 136
[12] Perumal P, Christopher Selvin P and Selvasekarapandian S 2018 *Ionics*
[13] Shukur M F, Yusof Y M, Zawawi S M M, Illias H A and Kadir M F Z 2013 *Phys. Scr. T* **157** 014050
[14] Sit Y K, Samsudin A S and Isa M I N 2012 *Res. J. Recent Sci.* **1** 16
[15] Mohamed N S, Subban R H Y and Arof A K 1995 *J. Power Sources* **56** 153
[16] Dodi G, Hritcu D and Popa M I 2011 *Cellul. Chem. Technol.* **45** 171
[17] Dufficy M K, Khan S A and Fedkiw P S 2015 *J. Mater. Chem. A* **3** 12023
[18] Carvalho D V, Loeffler N, Hekmatfar M, Moretti A, Kim G-T and Passerini S 2018 *Electrochim. Acta* **265** 89
[19] Liu J, Zhang Q, Zhang T, Li J-T, Huan L and Sun S-G 2015 *Adv. Funct. Mater.*
[20] Sudhakar Y N, Selvakumar M and Krishna Bhat D 2013 *Mater. Sci. Eng. B* **180** 12
[21] Johansson J P 1998 *Conformations and vibration in polymer electrolytes Thesis Dissertation* (Uppsala University, Sweden)
[22] Ramesh S, Liew C-W and Arof A K 2011 *J. Non-Cryst. Solids* **357** 3654
[23] Arof A K, Osman Z, Morni N M, Kamarulzaman N, Ibrahim Z A and Muhamad M R 2001 *J. Mater. Sci.* **36** 791
[24] Chitra R, Sathya P, Selvasekarapandian S, Monisha S, Moniha V and Meyvel S 2018 *Ionics*
[25] Polu A R, Rhee H-W and Kim D K 2015 *J. Mater. Sci.: Mater. Electron.*
[26] Baskaran R, Selvasekarapandian S, Kuwata N, Kawamura J and Hattori T 2006 *Solid State Ionics* **177** 2679
[27] Manjuladevi R, Christopher Selvin P, Selvasekarapandian S, Shilpa R and Moniha V 2018 *AIP Conf. Proc.* **1942** 140075
[28] Ramesh S and Soon C-L 2008 *J. Power Sources* **185** 1439
[29] Mudgil D, Barak S and Khatkar B S 2012 *Int. J. Biol. Macromol.* **50** 1035
[30] Liew C-W, Ng H M, Numan A and Ramesh S 2016 *Polymers* **8** 179
[31] Hodge R M, Edward G H and Simon G P 1996 *Polymers* **37** 1371
[32] Monisha S, Mathavan T, Selvasekarapandian S, Milton Franklin Benial A, Aristatil G, Mani N *et al* 2016 *Carbohydrate Polymers* 1
[33] Karthikeyan S, Sikkanthar S, Selvasekarapandian S, Arunkumar D, Nithya H and Kawamura J 2016 *J. Polym. Res.* **23** 51
[34] Boopathi G, Pugalendhi S, Selvasekarapandian S, Premalatha M, Monisha S and Aristatil G 2016 *Ionics*